

Theory of Percolative Conduction in Polycrystalline High-temperature Superconductors

Robert Haslinger and Robert Joynt

*Department of Physics and Applied Superconductivity Center
University of Wisconsin-Madison
1150 University Avenue
Madison, WI 53706
(May 3, 2017)*

Conduction in bulk polycrystalline high- T_c superconductors with relatively high critical currents has been shown to be percolative. This phenomenon is due to weak links at grain boundaries. These weak links are the major limiting factor for technological applications which require high current densities. We formulate a model of these materials which can be reduced to a nonlinear resistor network. The model is solved by analytical approximations and a new numerical technique. The numerical technique is variational, which makes it capable of solving a wide variety of nonlinear problems. The results show that the presence of a distribution of critical currents in the sample does not erase all information about the dissipative electrical properties of individual boundaries. This means that an unambiguous connection can be made between the $I - V$ characteristics at the microscopic level and the macroscopic electrical properties.

PACS Nos. 74.25.Fy, 74.62.Bf, 74.60.Jg, 74.72.-h

I. INTRODUCTION

The discovery of high- T_c superconductivity raised hopes of an important role for these materials in applications requiring high current densities, such as high-field magnets and transmission lines. The most important factor limiting current densities in present-day low- T_c materials is flux motion, and the solution is to maximize pinning. While this is important in the high- T_c materials as well, an even more vexing problem is that of weak links. Practical materials are polycrystalline: grain boundaries and other extended defects are unavoidable. These boundaries, usually not important in low- T_c materials, limit the flow of supercurrent in high- T_c systems. While bulk samples may be superconducting at low current densities, their critical currents are low. Since a transport current must pass through many of these boundaries, they pose a crucial problem in conductor development.

Experimentally, early work on grain boundaries showed that their critical currents I_c could vary over orders of magnitude [1]. Under these conditions, it might be expected that supercurrent flow in polycrystalline samples, at least near the critical current, would be percolative in nature. Recent work using magneto-optic methods has confirmed this. Particularly striking is work on BSCCO/Ag tapes [2]. As a result, one must understand the behavior of current flow when a *distribution* of boundaries is present, with possibly a wide spread in I_c .

On the theoretical side, percolation theory has dealt mainly with linear circuit elements and focused on the critical behavior (*i.e.*, power laws) near the percolation threshold [3]. Some work has been done with nonlinear elements. An example is the case of a lattice of resistive

elements with arbitrary nonlinearity [4], [5] where individual resistive elements are removed at random. The $I - V$ characteristic can be shown via renormalization group theory to follow a power law behavior near the percolation threshold. These renormalization group calculations do not tell us anything about the value of the critical current, or the shape of the $I - V$ characteristic away from the critical region. Some work away from threshold has been done for metal-insulator problems [6]. This problem is in a certain sense dual to the superconductor-metal problem studied in this paper, but the exact relation is not clear. The case of a linear medium containing a small admixture of nonlinear elements has also been studied. This model has applications in the study of composites formed of nonlinear impurities embedded in a linear host [7], [8], [9]. Theoretical predictions of $I - V$ characteristics are made using the Clausius-Mossotti approximation [7], or the effective medium approximation [8]. These are limited to the case of weak nonlinearity or a low density of nonlinear impurities.

The critical phenomena approach and the weak nonlinearity case are not closely relevant to our goal here, which is to understand the entire $I - V$ characteristic of a strongly nonlinear system. More closely related is the work of Leath and Tang. These authors first considered a Ginzburg-Landau model of conduction in polycrystalline superconductors, and later a simpler nonlinear resistor network [10]. The latter have generally been the more popular since then, since they provide a reasonable and relatively simple representation of the physical properties of a superconductor with weak links. Hinrichsen *et al.* considered a model which is a special case of the ones we shall treat [11], and it will be discussed further below. Our goal is different from both these papers, however. It

lies in determining the connection of the "microscopic" distribution of link strengths to the macroscopic $I - V$ characteristic. That is, we are interested not in a particular underlying model, but rather in determining what that model is, given global information. Hence we look for solution methods which will apply to whole classes of models, and which therefore amount to generalizations of those which have been discovered to date.

II. THE MODEL

The current flows through a random array of microcrystallites separated by grain boundaries which act as weak links. In this paper, we shall restrict our attention to the two-dimensional case - a granular superconducting film. There is nothing which prevents the generalization of any of the arguments to higher dimensions. The computational method we use is independent of dimensionality.

The first step is to construct an equivalent resistor network. For the purposes of simplicity we shall assume that each grain is perfectly conducting. This allows one to separate, at least temporarily, the two current-limiting factors (flux pinning and weak links) mentioned above. It means that our results are limited to cases in which the total magnetic field (applied plus self) is small enough that there is no flux penetrating into the grains. Flux only penetrates the boundaries.

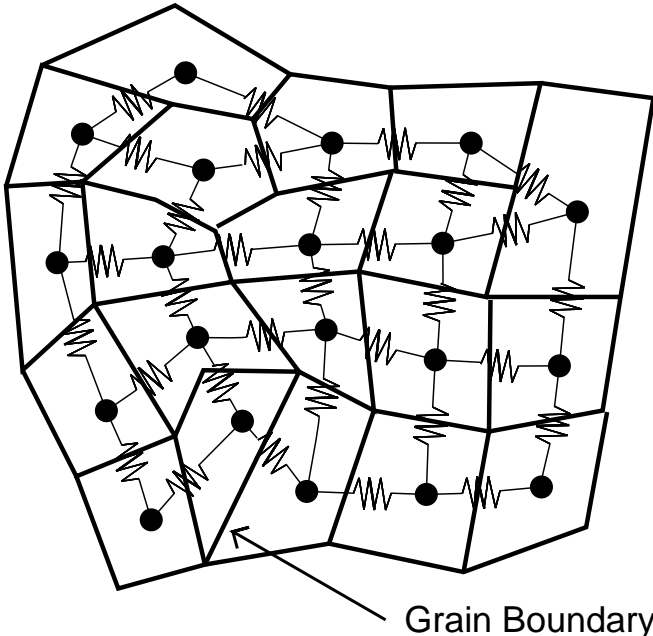


FIG. 1. Reduction of a polycrystalline superconducting network to an equivalent resistor network. The irregularly shaped regions are superconducting grains, taken as equipotentials. All potential drops take place across grain boundaries, shown as (nonlinear) resistors.

Once the grains are taken as perfectly conducting, then they are equipotential areas. They are the nodes of the network. Each pair of grains is separated by a boundary. Each boundary is replaced by a (nonlinear) resistor. An example of this construction is shown in Fig. 1. In graph-theoretical terms, the graph of boundaries is replaced by its dual graph. A theorem from topology [14] states that this relation is one-to-one. We shall suppose that the geometrical randomness is less important than the randomness in the strength of the resistors. Accordingly, we shall consider only square lattice networks.

Although we will develop techniques applicable to resistive elements of arbitrary nonlinearity, our main interest in this paper is the flow of current through a granular superconductor. Accordingly, we focus in this paper on two models of the grain boundaries applicable to the cases of Josephson junctions in low and high applied fields. Why actual boundaries should behave in these ways is discussed by Likharev [16].

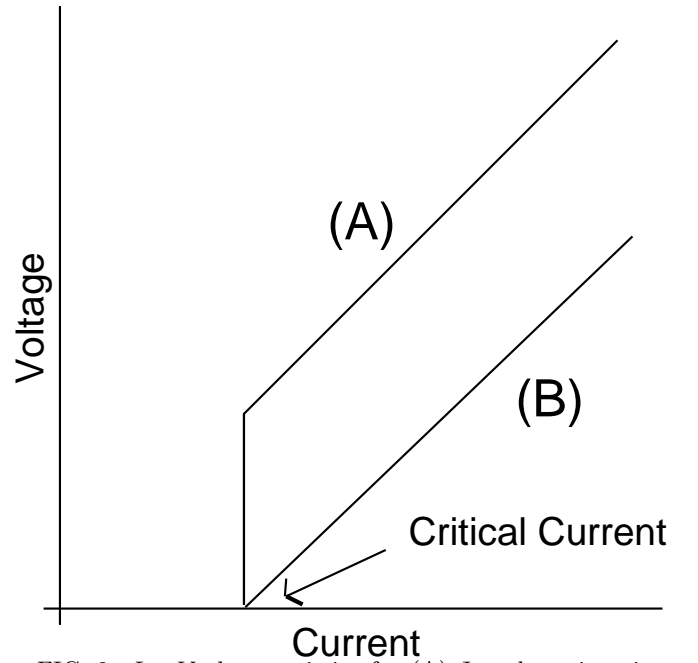


FIG. 2. $I - V$ characteristics for (A) Josephson junction (JJ) and (B) flux flow (FF) models. The former is considered to be appropriate for low fields, and the latter for high fields. In the numerical calculations, we give the JJ characteristic a finite slope just above the critical current for numerical stability.

Each boundary is specified by its $I - V$ characteristic. V is some nonlinear function of I for each resistor, but each resistor may be different. In the general case, the resistors are drawn from a probability distribution $\mathcal{P}[V(I)]$. We will concentrate on binary distributions, since the results easiest to understand. These binary distributions consist of a mixture of weak links and strong links, each weak link being identical, and each strong link being identical. The concentration of weak links will be

denoted by p and the concentration of strong links by $q = 1 - p$.

We further divide our model into two classes corresponding to weak-field Josephson junction (JJ) and strong-field flux flow (FF) boundaries. For the JJ case, the weak links, with concentration p , have a critical current I_{c1} . If $I < I_{c1}$ in such a resistor, then $V = 0$. If $I > I_{c1}$, then $V = IR_1$, where R_1 is a constant. Similarly, the strong links, with concentration $1 - p$, satisfy: if $I < I_{c2}$, then $V = 0$; if $I > I_{c2}$, then $V = IR_2$. $I_{c2} > I_{c1}$. Note that V is a *discontinuous* function of I for both types of links. Let us call this the binary JJ model. For the FF case, the weak links, with concentration p , have a critical current I_{c1} . For $I < I_{c1}$, $V = 0$. For $I > I_{c1}$, $V = (I - I_{c1})R_1$, where R_1 is a constant. The strong links, with a concentration $1 - p$, satisfy: if $I < I_{c2}$, then $V = 0$; if $I > I_{c2}$, then $V = (I - I_{c2})R_2$. $I_{c2} > I_{c1}$. Note that V is a *continuous* function of I for both types of links. This is the binary FF model. See Fig. 2 for an illustration of the two cases.

The two models represent very different microscopic pictures. The JJ model represents a low-current, zero applied field situation. The junction is taken as the simplest sort of Josephson junction. It is superconducting for small currents. It is normal at high currents and the voltage drop is just ordinary Ohmic loss. There is a discontinuous change between the two regimes. The FF model is intended to simulate a situation in which the links are weak because flux pinning in them is weak. In this case, I_c of the link represents the depinning current. The losses for $I > I_c$ are from the movement of flux along the boundary. Experimental measurements on individual grain boundaries show a cross-over between the two sorts of behaviour. Fig. 3 shows $I - V$ characteristics for a 10 degree grain boundary. At low applied field, the boundary resembles our JJ model, while at high field it is closer to the FF model.

As to the more fundamental issue of whether our model is really valid for superconductors, we note that the main missing element is the phases of the grains. This may not be as bad an approximation as at first sight, however. Our nonlinear network can be considered as an approximation to a true Josephson junction array in the overdamped limit. The JJ model can represent a set of overdamped junctions with no pinning in which the McCumber parameter $\beta_J \equiv \hbar R^2 / (2e I_{c0} C)^{1/2}$ is less than 1. R and C are the resistance and capacitance of the junctions. Our output I_{tot} then represents the DC component of the actual output of real overdamped junctions. The FF model is the case where pinning of Josephson vortices dominates the transport.

The output of our calculations will be a $V_{tot}(I_{tot})$ relation for the system as a whole. Thus, we feed a fixed current in at one end and collect it at the other, and measure the voltage drop. We wish to compare this result to experimentally measured $I - V$ characteristics such as that shown in Fig. 4 and determine the extent to which the percolation is responsible for the macroscopic

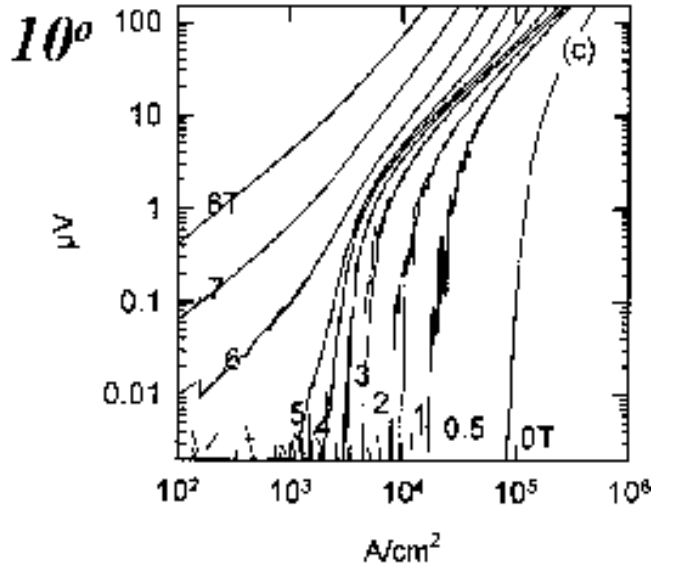


FIG. 3. Experimentally measured $I - V$ characteristics for a 10 degree YBCO grain boundary at various applied fields. At low fields, the $I - V$ characteristic resembles our JJ model. As the applied field increases, there is a crossover at 5.5 T to a behavior which is similar to our FF model. Data courtesy of N. Heinig and D.C. Larbalestier.

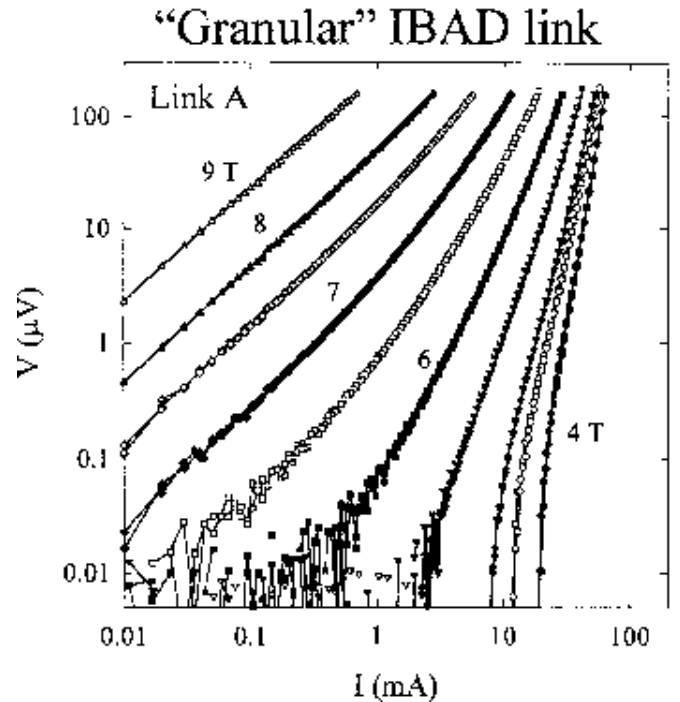


FIG. 4. Experimentally measured $I - V$ characteristics for IBAD film at various applied fields. Again there is a crossover at roughly 5.5 T. As in our model (Fig. 9) the *shape* of the individual grain boundaries $I - V$ is preserved in the macroscopic system. Data courtesy of N. Heinig and D.C. Larbalestier.

electrical properties and in particular, the critical current. In particular, we wish to understand whether the

presence of randomness and nonlinearity washes out most of the information about the individual resistors.

III. ANALYTICAL APPROXIMATIONS

In this section, we present an analytic approximation for the critical current of a binary lattice. Suppose we have a distribution of nonlinear resistors on an infinite lattice with each resistor possessing some critical current and occupation probability. (We shall take a lattice constant of unity to avoid distinguishing between currents and current densities.) This implies that the critical current can be found from the prescription:

$$I_{ctot} = \min_S \sum_{\ell \in S} I_c^{(\ell)}, \quad (1)$$

where we take the minimum over *all* surfaces which separate the electrodes [12]. ℓ are the wires which pierce S , and $I_c^{(\ell)}$ is the critical current of wire ℓ . This explicit but highly formal equation does not give any prescription for computation of I_{ctot} except in very small systems. It says only that the network is only as strong as its weakest hypersurface; in two dimensions, its weakest curve. However, because I_{ctot} depends only on $I_c^{(\ell)}$, Eq. 1 tells us that the total critical current of the lattice depends only upon the critical currents of the individual elements and not upon their dissipative behaviour at $I > I_c$.

Consider two adjacent infinite surfaces S and S' , both of which separate the electrodes. The maximum supercurrent which can be carried through S , considered entirely by itself, is clearly

$$I_c^{(\infty)} = \sum_j p_j I_{cj}. \quad (2)$$

However, it is not clear that the current can penetrate from S to S' . Indeed we expect the critical current of the infinite lattice to be less than $I_c^{(\infty)}$, which serves as an upper bound for I_{ctot} , independent of model and dimensionality.

To obtain a better approximation for I_{ctot} , consider a binary model, where there are only two types of resistors I_{c1} and I_{c2} with occupation probabilities p and $q = 1 - p$ respectively. Since we are only interested in the critical current, the exact $I - V$ characteristic of these resistors is unimportant. For this model the bound of Eqn. 2 is $I_c^{tot} = pI_{c1} + qI_{c2}$. As q increases, there will be a large increase in the critical current when $q > p_c$. This is obvious since for $q > p_c$ we get an infinite cluster of I_{c2} resistors running through the lattice, allowing much more current to be transported. However, it is **not** true that $I_{ctot} = I_{c1}$ for $q < p_c$. This is most easily understood in the following manner.

Consider an $M \times N$ square lattice and suppose there is a current $I > NI_{c1}$ transported horizontally across the lattice. Due to the geometry of the lattice, we divide

the resistors into two groups. We will call those resistors running perpendicular to the average current flow "row resistors" and term a line of these to be a "row". The rows are connected by what we will call "column resistors" and the resistors connecting two rows make up a "column", as shown in Fig. 5. The current flow can be considered a superposition of two current distributions, NI_{c1} running directly through the lattice (along the column resistors), and a percolating current $I - NI_{c1}$. It is this percolating current that we are interested in, so we can "subtract off" an I_{c1} resistor from each column resistor. A modified dilute resistor network lattice results and is shown in Fig. 5. The columns of this lattice have holes with probability p , and $I_{c3} = I_{c2} - I_{c1}$ critical current resistors with probability $q = 1 - p$. This modified lattice has a critical current I_{cM} . The total critical current is then $I_{ctot} = I_{c1} + I_{cM}$.

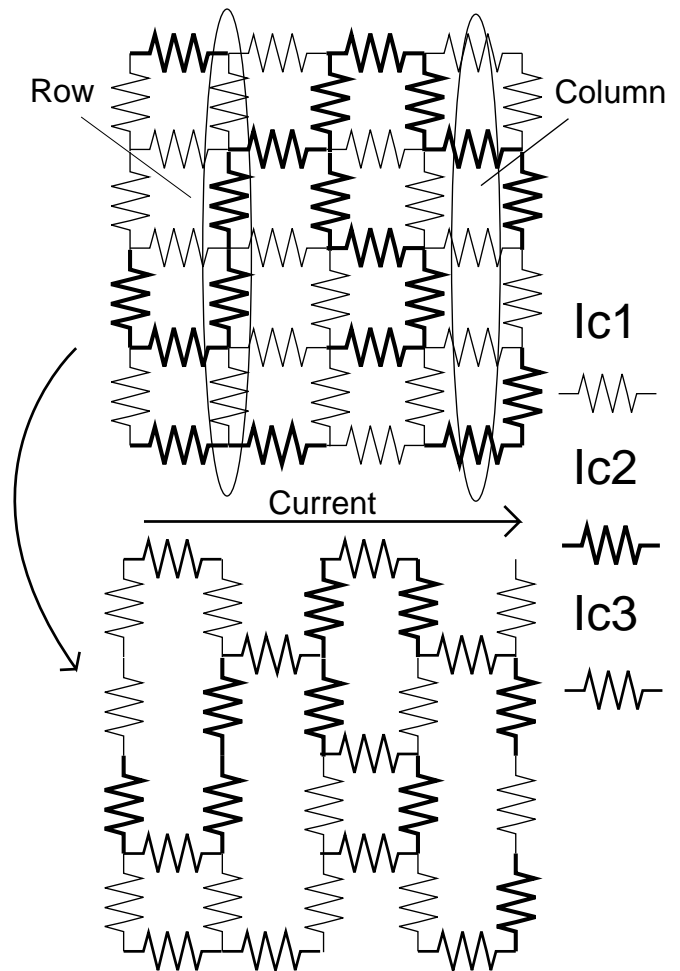


FIG. 5. Picture of a two-dimensional network. The current runs to the right. We divide the resistors into those parallel to the current (column) and perpendicular (row). The actual lattice is then reduced to a dilute network by subtracting out a uniform current to the right.

I_{cM} is determined by two factors. First, the amount of current that can be transported across any given column

of the lattice, and second, whether or not that current can be redistributed to the I_{c3} resistors in the next column. There are two different regimes of behavior distinguished by whether I_{c3} is less or greater than I_{c1} . The first case is simplest.

When $I_{c3} < I_{c1}$ ($I_{c2} < 2I_{c1}$), it is fairly easy to redistribute the current between columns. Any current coming across a column resistor can be shunted sideways along a row and redistributed to the next column as long as another column current doesn't get in the way. We can approximate the probability that a given column current can be redistributed along a row without being interfered with in the following fashion. It is equal to the probability that there is an I_{c3} resistor directly across from the given column current, plus the sum of probabilities that there is a path at a site s steps along the row, and no paths either coming in or out of the row before that point. By only summing over steps to the right (or left) of the given column current, we avoid the problem of interfering with the paths of other incoming column currents. This redistribution probability can then be written as:

$$p_r = q \times \sum_{s=0}^{\infty} (1-q)^{2s} = \frac{q}{2q - q^2} \quad (3)$$

Since we have a volume fraction q of I_{c3} row currents, we can then write down the averaged critical current density as:

$$\begin{aligned} I_{ctot} &= I_{c1} + (I_{c2} - I_{c1}) \times q \times p_r \\ &= I_{c1} + (I_{c2} - I_{c1}) \times \frac{q^2}{2q - q^2}. \end{aligned} \quad (4)$$

It should be evident that this is only an approximate formula. The derivation neglects the possibility that the percolation current goes backward, for example. However, we expect this path to make a smaller contribution than the ones calculated, since they must involve relatively rare configurations of resistors.

A plot of Eq. 4 for a 15 by 15 lattice is shown in Fig. 6, where the results are compared to numerical data. It appears to overshoot the critical current by a substantial amount. We will see, however, that this is due to the finite size of the lattice used (15 by 15). For the infinite lattice case, the approximation should be very good if $I_{c3} < I_{c1}$.

If $I_{c3} > I_{c1}$ then this calculation will fail, since it is no longer as easy to shunt the current sideways along a row of resistors, and hence the redistribution probability will be different. A calculation similar to that above gives a different critical current:

$$I_{ctot} = I_{c1} + q\{I_{c1}(p_r - p'_r) + (I_{c2} - I_{c1})p'_r\} \quad (5)$$

where:

$$p'_r = q \times \sum_{s=0}^{\infty} (p^2 q)^s = \frac{q}{1 - p^2 q} \quad (6)$$

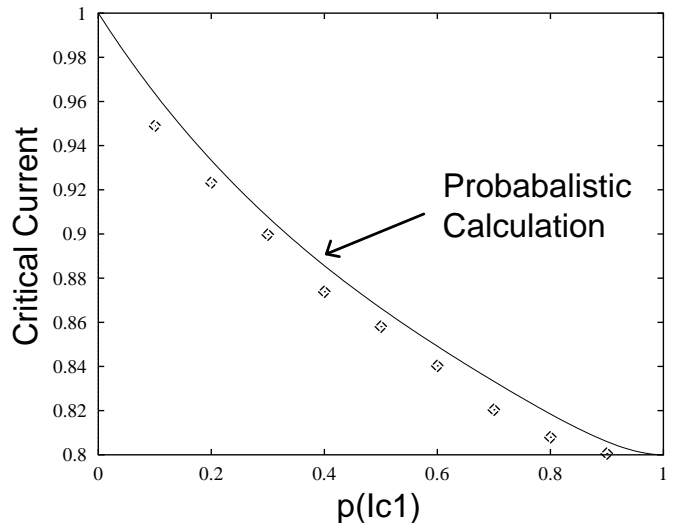


FIG. 6. Comparison of probabilistic theory to numerical data. The critical current for a square lattice where $I_{c1}/I_{c2} = 0.8$ is approximated for varying occupation probabilities p and compared with the numerical data for a 15×15 lattice.

While this analysis can clearly be extended to distributions of more than two resistors, it quickly becomes much more complicated. In addition, it tells us nothing about dissipative behaviour at currents greater than I_{ctot} . Hence we now turn to numerics.

IV. NUMERICAL CALCULATIONS

Assume that we have a nonlinear resistor network and that the distribution of resistive elements is known. If a current is imposed across the network, a voltage drop results. We wish to calculate this voltage drop for the entire lattice. The correct distribution of currents in the lattice can be found by solving Kirchoff's equations, which uniquely determine the current distribution in the network. In a network of linear resistors, this reduces to solving a set of linear equations, for which many standard methods exist. For nonlinear resistors, we are not aware of any general method. The method of Leath and Tang [10], also used by Hinrichsen *et al.*, [11], works only for the JJ case. The approach we take is to search among all distributions of current which satisfy current conservation and transport the imposed current across the lattice. We then determine which distribution in this class also has a unique voltage at each node.

To search among all current distributions in this class, we begin by choosing a distribution which is thought to be close to the actual one. This choice must conserve current at each lattice node, and must also transport the imposed current across the lattice. One possibility would be a distribution where the current moves uniformly across the lattice. This initial guess obviously needs to be modified. We do this by superimposing circulation currents on

top of the initial distribution as shown in Fig. 7. While these circulation currents contribute nothing to the net transport of current, they alter the path that the current takes. Current conservation is obviously satisfied for all values of the circulation currents. The circulation currents have become our free variables. It is an elementary result of homology theory [14] that all circulating currents can be generated by the addition of currents circulating around plaquettes. Thus our search method can ultimately produce all possible currents.

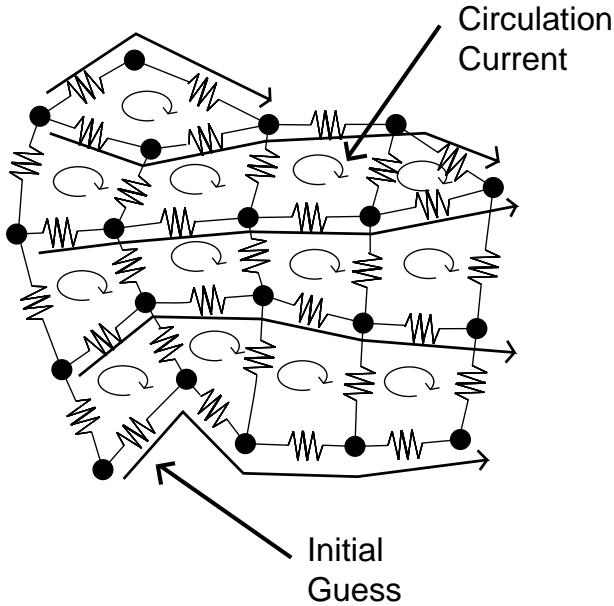


FIG. 7. Initial guess for the current distribution and imposition of circulation currents

The current distribution satisfying the voltage Kirchoff law must still be found. We note that this requirement can be expressed in terms of a minimization principle. If, for a given resistor, we define the quantity:

$$g_j = \int_0^{I_j} V_j(i) di \quad (7)$$

where $V_j(i)$ is the voltage-current characteristic of the j th resistor (which we assume to be known) and I_j is the current flowing through the j th resistor, then solving Kirchoff's laws is equivalent to minimizing:

$$\mathcal{G} = \sum_j g_j \quad (8)$$

where the sum is over all resistors in the lattice. We prove this by varying \mathcal{G} with respect to the currents such that current conservation is preserved. That is, vary \mathcal{G} with respect to a circulation current:

$$\frac{\delta \mathcal{G}}{\delta C_k} = \sum_j V(I_j) \frac{\delta I_j}{\delta C_k} = 0 \quad (9)$$

Since the circulation current C_k travels around a specific loop, variations in C_k only affect the currents along that loop. In addition the effect is unit linear in C_k .

$$\begin{aligned} \frac{\delta I_j}{\delta C_k} &= 1 \text{ (} I_j \text{ on loop } k \text{)} \\ \frac{\delta I_j}{\delta C_k} &= 0 \text{ (otherwise)} \end{aligned} \quad (10)$$

where the sign is positive in the direction of C_k . Then,

$$\frac{\delta \mathcal{G}}{\delta C_k} = \sum_{j \in \text{loop}} V_j = 0 \quad (11)$$

This is valid for any loop in the lattice and hence we see that the minimization of \mathcal{G} with respect to the circulation currents is equivalent to solving Kirchoff's voltage law. It is interesting to note that in the case of linear resistors, \mathcal{G} reduces to $\mathcal{G} = (1/2) \sum_j R_j I_j^2$. So for the linear case, or indeed any network where all the voltages have the same power law dependence upon current, minimizing \mathcal{G} is equivalent to minimizing the power loss of the lattice, a familiar result.

It seems unlikely to us that this variational principle for nonlinear systems is not known. However, we have not been able to find it in the literature. We note that this method is not at all limited to this electrical example. It should be applicable to nonlinear transport of any conserved quantity. Fluid flow in random porous media is one candidate.

Due to its robustness and applicability to highly disordered systems with many variables we chose a simulated annealing algorithm to perform the minimization. Determining whether an optimization algorithm has found the global minimum can be difficult. However, in the nonlinear percolation case with monotonic $I - V$ relations, a check can be made. At the global minimum, the voltage drop across the lattice should be a constant regardless of the path taken. By calculating the voltage drop along various paths, the accuracy of the solution can be determined.

The main advantage of this algorithm is its generality. It is immediately applicable to elements of *arbitrary* nonlinearity, as well as any geometrical arrangement of these elements. We also note that this algorithm supposes an imposed *current* across the lattice. An equivalent minimization principle for an applied voltage can be formulated by minimizing the sum:

$$\sum_j h_j = \sum_j \int_0^{V_j} I_j(v) dv \quad (12)$$

where the sum is over the resistors, and the free variables are the voltages at each node [4].

While we are mainly interested in the infinite lattice case, realistically we must work with lattices of finite size. While one generally approximates the infinite case by averaging over many small lattices, the finite size fluctuations can still be important.

To understand the effect finite size has on the critical current, take a binary model on a square lattice. Eq. 2 gave us the bound

$$I_{c1} \leq \frac{I_{ctot}}{N} \leq pI_{c1} + (1-p)I_{c2} \quad (13)$$

for an infinite lattice. However, for a finite lattice, this upper bound decreases. For a $N \times N$ lattice of nodes, we have a resistor lattice with $M = N - 1$ columns and N resistors in each column Fig. 5. We are interested in the fluctuations. The occupation probabilities may be p and $q = 1 - p$, but we are obviously going to see large fluctuations from the mean in a smaller lattice. So what we want is the expectation value for the maximum number of I_{c1} resistors in any of the M columns, since this will be the limiting factor on the critical current. In order to find this expectation value, we need the probability $\mathcal{P}(a)$ that the maximum number of I_{c1} resistors in any of the $M = N - 1$ columns is a (out of N).

To derive an expression for $\mathcal{P}(a)$, define $f(a)$ to be the probability that a specific column has ' a ' I_{c1} 's in it. Then

$$f(a) = \frac{N!}{a!(N-a)!} p^a (1-p)^{N-a}. \quad (14)$$

Now define $P_M(x, a)$ as the probability that x columns (out of M) have a I_{c1} resistors in them.

$$P_N(x, a) = \frac{M}{x!(M-x)!} f(a)^x (1-f(a))^{M-x} \quad (15)$$

where $0 \leq x \leq M$. $\mathcal{P}(a)$ is then given by:

$$\begin{aligned} \mathcal{P}(a) &= \sum_{x=1}^M [P_M(x, a) \times \prod_{i=a+1}^N P_{M-x}(0, i)] & a \neq N \\ \mathcal{P}(N) &= \sum_{x=1}^M P_M(x, a) & a = N \end{aligned} \quad (16)$$

The above equation is simply the probability that x columns in M have a R_1 resistors, multiplied by the probability that there are no columns (in the $M-x$ remaining) that have more than a R_1 resistors in them, summed over x .

We then use $\mathcal{P}(a)$ to find the expectation value of a :

$$\bar{a} = \frac{\sum_{a=0}^N a \mathcal{P}(a)}{\sum_{a=0}^N \mathcal{P}(a)} \quad (17)$$

Finally we get the critical current for the lattice,

$$I_{ctot} = \frac{\bar{a}I_{c1} + (N - \bar{a})I_{c2}}{N} \quad (18)$$

This analysis is only relevant for small lattices, since for very large lattices \bar{a} will be very close to p . However, for smaller lattices this effect can indeed be the limiting factor, as can be seen by looking at Fig. 8 where we plot the critical current for a 15 by 15 lattice with $I_{c1} = 0.8$ and $I_{c2} = 1.0$ for various occupation probabilities. The critical current is limited by the finite size of the lattice and that the critical current for the infinite case would be larger.

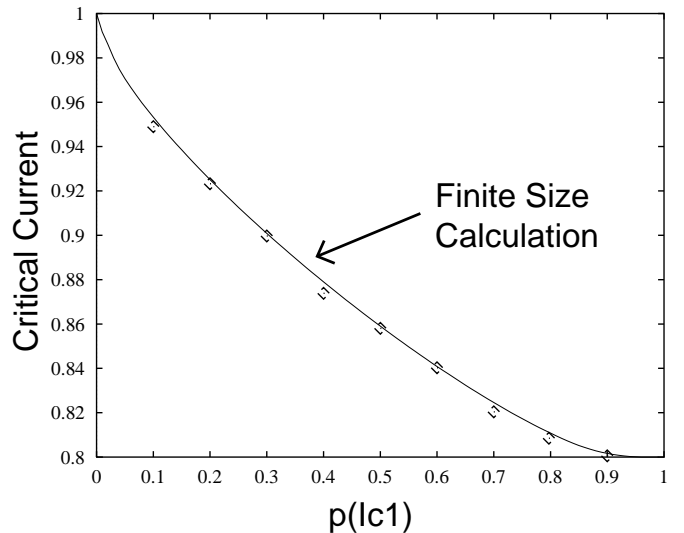


FIG. 8. Finite size calculation. $I_{c1}/I_{c2} = 0.8$ The limiting effects of finite size on the critical current are calculated for a 15×15 square lattice and compared with the numerical results.

V. $I - V$ RELATIONS

The current-voltage characteristics of both JJ and FF binary models were studied. For the sake of computational ease, the calculations were performed on square lattices, usually 10 by 10. The $I - V$ characteristics from 50 lattices were averaged to obtain the final result. It should be noted that the JJ $I - V$ characteristic used in the calculations is slightly modified from that which was previously discussed. Instead of a strictly discontinuous model, the transition at I_c from $V = 0$ to $V = IR$ was made to be linear over a small current range δI . In addition to being more physically realistic, this modification made the convergence of the simulated annealing algorithm much quicker.

The most important result of the numerical simulations is that the overall shape of the individual elements V-I characteristics is preserved when the elements are combined into a lattice. Fig. 9 compares a 10 by 10 lattice composed of JJ resistors with one of FF. $p = 0.5$, $I_{c1}/I_{c2} = 0.75$ and $R_1/R_2 = 0.75$ in both cases. We see that the resulting overall characteristics are very different. This in itself is not surprising as the individual components have different properties. However, the fact that the overall characteristics should resemble that of the individual elements so closely is surprising. Statistical averaging, even with strong nonlinearity, does not wash out the underlying input.

Since both JJ and FF resistors are linear at high current, it is clear that the collective behavior of a lattice of resistors will be linear at high currents. In addition, the slope (conductivity) will be independent of the model used. We also expect that this high current behavior of the JJ and FF V-I curves is offset vertically, so that for

JJ we expect the voltage to go as $V = IR$ and for FF, $V = (I - I_c^{\text{eff}})R$. ($I_c^{\text{eff}} \neq I_{ctot}$ necessarily) This can be seen in Fig. 9. The nature of the transitions between the superconducting and the high current behavior as well as the current range over which the transition should occur is not as evident.

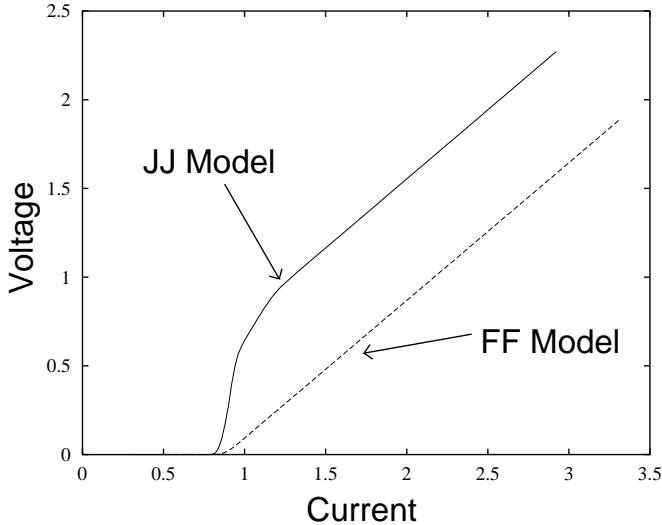


FIG. 9. Comparison of the $I - V$ characteristics for binary JJ and FF models on a 10 by 10 percolative lattice. Both models possess the same distribution of microscopic critical currents and normal state resistances. ($I_{c1}/I_{c2} = 0.75$, $R_1/R_2 = 0.75$, $p = 0.5$) The *shape* of the individual circuit elements $I - V$ characteristics is preserved when they are combined into a lattice.

Our calculations show that the net transition behavior closely mimics that of the individual elements. Qualitatively, we believe the explanation is as follows. While I_{ctot} is independent of the choice of model, as there is no difference in the behaviour of JJ and FF resistors below I_c , the behaviour above I_{ctot} is highly model dependent. FF resistors can conduct at all voltages, and hence the transition from superconductivity to dissipative conduction for a FF lattice is smooth and gradual. However, the JJ resistors have an almost discontinuous jump in resistance at I_c . It is harder to satisfy Kirchoff's laws at low voltages, since these low voltages are in effect "forbidden". Thus the rise in voltage at I_{ctot} is very steep, and the breadth of the transition rather narrow.

Exactly how narrow the transition to dissipative behaviour is depends on the probability distribution of the critical currents. For the binary model, as $I_{c2} - I_{c1}$ grows, the transition broadens. This is true for both JJ and FF, (although it is easiest to see in the JJ case). We illustrate this in Figs. 10 and 11 where the effects of varying I_{c1}/I_{c2} for lattices of fixed occupation probability p ($q = 1 - p$) and fixed R_1/R_2 for both JJ and FF lattices are shown. If on the other hand we vary the occupation probability p as in Figs. 12 and 13, we see that the transition from superconductivity to the high current behavior is broadest at $p = 0.5$, and gets much narrower towards

$p = 0$ or 1. Thus we see that as the *probability distribution* for the critical currents of the individual elements flattens out, the current range occupied by the transition from superconductor, to normal conductor becomes much larger. This statement is still relevant for non-binary systems which have a distribution of $I - V$ characteristics $\mathcal{P}(V(I))$.

Very detailed comparison between theory and experiment is beyond the scope of this paper. It would require the experimental determination of the entire individual resistor distribution as well as macroscopic $I - V$ curves. However, we can get partial information about the former and compare to the latter as a preliminary exercise.

Fig. 3 shows $I - V$ characteristics measured across a single 10° grain boundary at various applied fields. Varying the magnetic field applied to a grain boundary will change the grain boundary's properties. The critical current, in general, decreases with increased applied field. The high current resistance is dependent on the applied field as well. We however wish to focus for now on the *shape* of the boundary's $I - V$ characteristic. At low fields the grain boundary displays a Josephson junction type behaviour which resembles our JJ model. At about 6 T there is a transformation to a different high field behaviour caused by the depinning of flux along the grain boundary. We modeled this high field behavior with our FF model.

How does a sample consisting of many grain boundaries behave? Fig. 4 gives the voltage current characteristics for a link comprised of many grain boundaries, made by ion-beam assisted deposition (IBAD). At low applied fields, the overall $I - V$ characteristic looks somewhat like a Josephson junction. As the field is increased the curvature of the characteristic changes at about 5 T, and it begins to look much more linear. It appears that the new dissipative behavior is dominated by flux creep as opposed to a Josephson type dissipation. Our resistor model supports this. We have shown through our resistor model that the microscopic single grain boundary (resistor) characteristics can (at least in the case of JJ and FF) be carried through by percolation to the macroscopic many grain boundary case. A macroscopic sample comprised of grain boundaries acting as Josephson junctions will itself have a very sharply rising $I - V$ characteristic, while a sample where the dissipation is dominated by flux creep will resemble its individual components as well.

Comparison of our theory with the experiment suggests that the grain boundaries dominate the dissipative properties of the macroscopic superconductor, *even in applied magnetic fields*. If this is the case, then the effects of the grains themselves are less important for the IBAD samples.

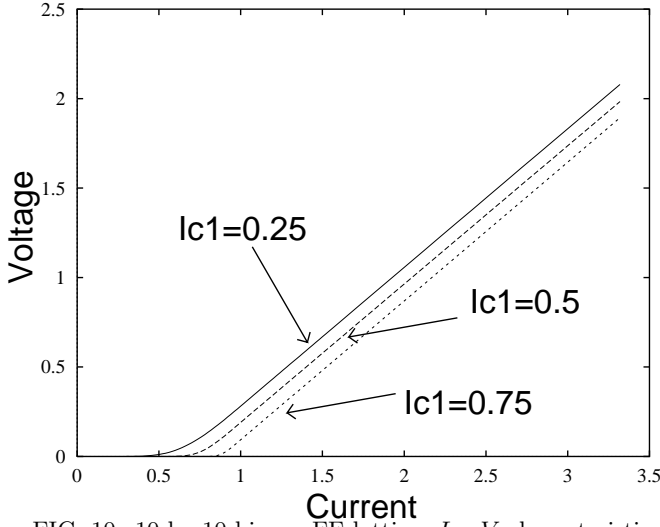


FIG. 10. 10 by 10 binary FF lattice. $I - V$ characteristics for various I_{c1}/I_{c2} are shown. $p(I_{c1}) = 0.5$, $R_1/R_2 = 0.75$

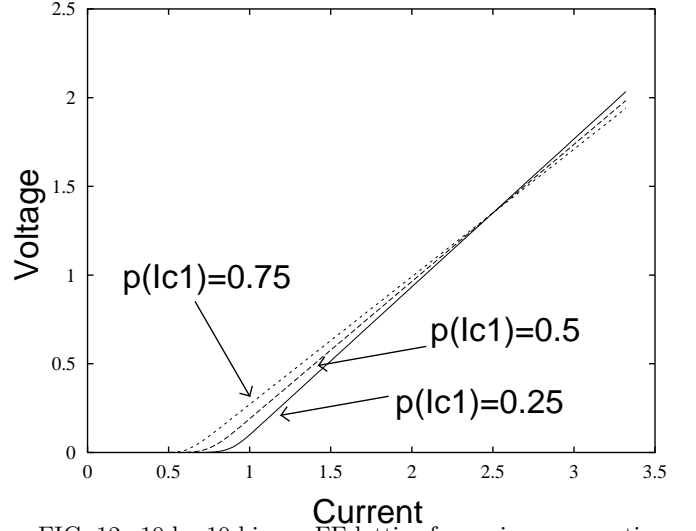


FIG. 12. 10 by 10 binary FF lattice for various occupation probabilities $p(I_{c1})$. $I_{c1}/I_{c2} = 0.5$, $R_1/R_2 = 0.75$

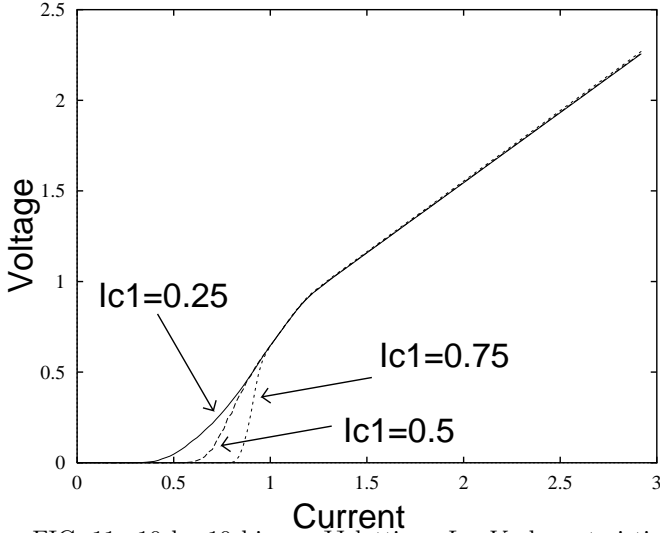


FIG. 11. 10 by 10 binary JJ lattice. $I - V$ characteristic for various I_{c1}/I_{c2} are shown. $p(I_{c1}) = 0.5$, $R_1/R_2 = 0.75$. There is substantial broadening of the transition near I_c due to the finite lattice size.

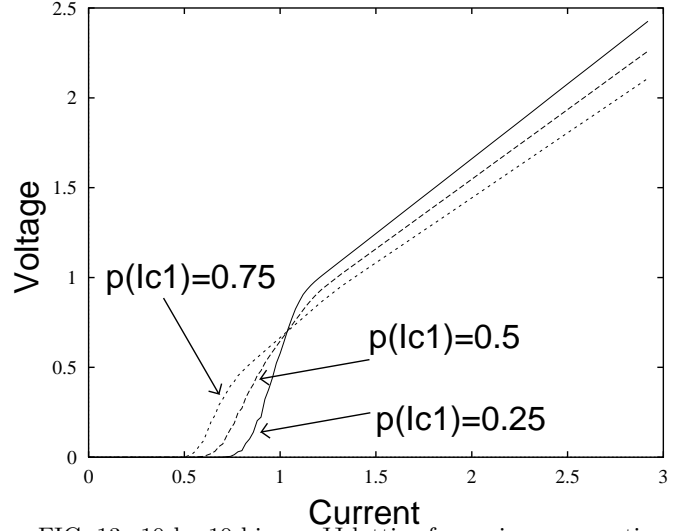


FIG. 13. 10 by 10 binary JJ lattice for various occupation probabilities $p(I_{c1})$. $I_{c1}/I_{c2} = 0.5$, $R_1/R_2 = 0.75$. Again, finite size transition broadening may be seen.

VI. CONCLUSION

Conduction in polycrystalline high- T_c superconductors is percolative, each percolative path being nonlinear. We believe that the model considered in this paper is general enough to capture the essence of this phenomenon. It requires powerful numerical techniques: the one introduced in this paper should be flexible enough to handle virtually any distribution of grain boundary conductances. For simple distributions, for example binary models, probabilistic reasoning can give insight into, and even good quantitative approximations for, the magnitude of the macroscopic critical current.

Not only the critical current is of interest for applications. One also wishes to know what the full $I - V$ characteristic is telling us about the properties of individual grain boundaries. What emerges from the calculations is that the *shape* of macroscopic current-voltage relation mirrors, to a remarkable extent, the *shape* of the underlying current-voltage relations of the grain boundaries. This is counterintuitive because the latter have a distribution which may be broad, and one would expect this to produce a broadening which would wash out discontinuous behavior near I_{ctot} . This does not happen. Nor does it happen that, for example, there is a two-step behavior for binary distributions. Instead, we find that the full $I - V$ always has nearly the same shape as the individual

$I - V$'s, but with parameters which are averages over the underlying distribution.

Our method allows us to find the full spatial distribution of current. We have not yet made use of this information. It is measurable by magneto-optical or Hall probe methods, and surely contains information about the spatial distribution of microscopic critical currents. This represents a possible future direction for this work.

We would like to thank A. Gurevich, E. Pashitskii, M. Friesen, N. Heinig, D. Cyr and D.C. Larbalestier for useful discussions. This work is supported by the NSF under Grant No. DMR-9704972 and under the Materials Research Science and Engineering Center Program, Grant No. DMR-96-32527.

-
- [1] D. Dimos, P. Chaudhari, J. Mannhart, and F.K. LeGoues, Phys. Rev. Lett. **61**, 19 (1988)
 - [2] A. Pashitskii, A. Polyanskii, A. Gurevich, J. Parrell, and D.C. Larbalestier, Physica C **246**, 133 (1995)
 - [3] J. Ziman, *Models of Disorder*, (Cambridge University Press, Cambridge, 1979), p. 370 ff.
 - [4] J. Straley and S. Kenkel, Phys. Rev. B **29** 6299 (1984)
 - [5] J. Straley and S. Kenkel, Phys. Rev. Lett. **49** 767 (1982)
 - [6] Y. Gefen, W.-H. Shih, R. Laibowitz, and J.M. Viggiano, Phys. Rev. Lett. **57** 3097 (1986); S. Roux and H.J. Herrmann, Europhys. Lett. **4** 1227 (1987); L. de Arcangelis and H.J. Herrmann, Phys. Rev. B **39** 2678 (1989)
 - [7] O. Levy and D. Bergman, J. Cond. Mat. **5** 7095 (1993)
 - [8] C. S. Yang and P. M. Hui, Phys. Rev. Lett. **44** 12559 (1991)
 - [9] H. Lee *et al.*, Phys. Rev. B **52** 4217 (1995)
 - [10] P.L. Leath and W. Tang, Phys. Rev. B **39**, 6485 (1989); P.L. Leath and W. Xia, Phys. Rev. B **44**, 9619 (1991)
 - [11] E. Hinrichsen, S. Roux, and A. Hansen, Physica C **167**, 433 (1990)
 - [12] J. Rhyner and G. Blatter, Phys. Rev. B **40**, 829 (1989); *ibid.*, Europhys. Lett. **10**, 401 (1989)
 - [13] M. Prester, Physica C **235**, 3307 (1994); *ibid.*, Phys. Rev. B **54**, 606 (1996)
 - [14] R. A. Armstrong, *Basic Topology*, (Springer, Berlin, 1983)
 - [15] S.E. Russek, D. Lathrop, B. Moeckly, R.A. Buhrmann, D. Shin, and J. Silcox, Appl. Phys. Lett. **57**, 1155 (1990)
 - [16] K.K. Likharev, Rev. Mod. Phys. **51**, 101 (1979)